United States Military Academy
USMA Digital Commons

Fall 11-15-2020

Spin Stabilization of an Air Ambulance Litter

Christopher Forden CDT'20
United States Military Academy, christopher.w.forden.mil@mail.mil

Yanuel Trinidad CDT'20
United States Military Academy, vazquez.y.trinidad.mil@mail.mil

Ryan von Chance-Stutler CDT'20
United States Military Academy, rvonchance@gmail.com

Andrew Bellocchio
United States Military Academy, andrew.bellocchio@westpoint.edu

James E. Bluman
United States Military Academy, james.bluman@westpoint.edu

See next page for additional authors

Recommended Citation
Forden, Christopher CDT'20; Trinidad, Yanuel CDT'20; von Chance-Stutler, Ryan CDT'20; Bellocchio, Andrew; Bluman, James E.; and Lanzerotti, Mary, "Spin Stabilization of an Air Ambulance Litter" (2020).

Authors

Christopher Forden CDT'20, Yanuel Trinidad CDT'20, Ryan von Chance-Stutler CDT'20, Andrew Bellocchio, James E. Bluman, and Mary Lanzerotti

Proceedings of the ASME 2020
International Mechanical Engineering Congress and Exposition
IMECE2020
November 15-19, 2020, Portland, OR, USA

IMECE2020-23386

SPIN STABILIZATION OF AN AIR AMBULANCE LITTER

Christopher Forden[1], Yanuel Trinidad[1], Ryan von Chance-Stutler[1], Andrew Bellocchio[1], James Bluman[1], Mary Lanzerotti[1]

[1]United States Military Academy, West Point, NY

ABSTRACT

This paper proposes a new approach to stabilize the spin of a suspended litter during air ambulance rescue hoist operations. Complex forces generated by the helicopter's downwash may cause a patient suspended in a rescue litter to spin violently. In severe cases, the spin destabilizes the suspended load, risks injury to the patient, and jeopardizes the safety of the aircrew.

The presented design employs an anti-torque device to arrest the spin that is safer and faster than a tagline and is without the tactical constraints of the tagline. The device follows tailored control laws to accelerate a flywheel attached to the litter, thereby generating sufficient angular momentum to counteract the spin and stabilize the suspended litter. An inertial measurement unit (IMU) measures the position, angular velocity, and angular acceleration of the litter and delivers this information to a microcontroller.

The research and prototype design were developed under the support of the U.S. Army 160th Special Operations Aviation Regiment (SOAR).

NOMENCLATURE

RPM	revolutions per minute
g-force	gravitational force equivalent
α	angular acceleration
I	mass moment of inertia
k_1	angular displacement controller gain
k_2	angular velocity controller gain
k_Θ	stiffness of rescue cable
L	angular momentum
m	mass
m_{eff}	effective mass of the system (in vibrations)
P	power
R_i	inner radius of flywheel
R_0	outer radius of flywheel
s	Laplace domain complex variable
t	time
τ	torque
ω	angular velocity
Θ	angular displacement
$\ddot{\Theta}$	angular acceleration

1. INTRODUCTION

In response to complex forces generated by a helicopter's rotor wash, an air ambulance litter attached to the bottom of a hoist (Figure 1) may spin aggressively. These occurrences must be controlled or otherwise prevented so that the patient and aircrew do not experience unnecessary dangers. The maximum g-force that a human can experience before the acceleration becomes damaging to the human body is close to 2-g of acceleration [1]. For a typical litter, the acceleration limit is exceeded by a spin rate of 42 rpm. An example of excess spin occurred in Piestewa Peak, Arizona in 2019, in which a 74-year-old hiker experienced a life-threatening air evacuation due to excess spin of her rescue litter. The spin reached a speed of 190 rpm [2] and became so extreme that the patient lost consciousness and received additional injuries.

Air ambulance rescues with hoists are frequently conducted over-water, in mountainous, or in restricted terrain that precludes landing [3]. Table 1 lists air ambulance rescues of note completed for civilian patients [1, 4-13].

TABLE 1: CUSTOMERS IN AIR AMBULANCE RESCUES

Civilian Customers	Date(s)	Locations
Hikers	2016-2019	Arizona, Washington, Death Valley, Georgia [1, 4, 5, 6]
Snow rescues	2016	Switzerland [7]
Holiday-makers on cruise ships	2018	North Carolina, New Caledonia [8, 9]
Kayakers	2019	British Columbia [10]
Water rescues	2018, 2016	Bering Sea, California [11, 12]
Logger	2016	Tillamook [13]

This material is declared a work of the U.S. Government and is not subject to copyright protection in the United States.
Approved for public release; distribution is unlimited.

Air rescues are also a military operation. U.S. Army medevac units and the 160th Special Operations Aviation Regiment (SOAR) utilize both the HH-60M Blackhawk and CH-47 Chinook helicopters with attached Breeze Eastern HS-29900 or HS-10300 rescue hoists for rescue operations [2]. As seen in Figure 1, current Army medevac operations employ a stokes litter that connect to a rescue hook below the helicopter [14]. The hoists are vital in air rescue operations as they allow for medevac helicopters to hover and extract injured personnel [15], [16]. Rescue operations carry high risk with one of the greatest dangers being litter spin.

FIGURE 1: PHOTOGRAPH OF THE GEORGIA NATIONAL GUARD CONDUCTING A MEDEVAC OPERATION [14]

1.1 Hazards of Litter Spin

Of the different types of rotor wash flow field structures, the U.S Army's Rotorwash Analysis Handbook [17] states the *wall jet* "has the greatest potential for creating hazards in close proximity to the ground" where the wall jet occurs "when high velocity downwash exits the plane of the rotor, impinges on the ground, changes direction by 90 degrees, and then accelerates radially outward." The maximum value of outward velocity is reached at approximately one rotor diameter from the rotor's axis of rotation" [14]. The positioning of aircraft relative to the ground frequently places the litter inside the wall jet and promotes litter spin. More risk to spinning events exists at cable lengths above 50 feet; however, spinning events can happen above or below. At higher altitudes, there is more time for the hoist load to be affected by aerodynamic forces, thereby increasing the potential for oscillations, or spinning [16].

The litter spin is a hazard to the patient and a rescuer suspended by the hoist. During extreme spinning, Scheuring *et al*. remarked [18] the spin's *head-to-toe* acceleration "primarily affect the circulatory and pulmonary system" by reducing the "effective cardiac output to the brain and movement of the column of oxygenated blood in the carotid arteries to the brain." Additionally, there is risk of shoulder injury to crew chiefs as they attempt to grab the litter and slow its spin while bringing it into the cabin [16].

1.2 Current Solutions and Capability Gaps

Both the HH-60M and especially the CH-47, have zones of disruption where downwash highly impacts the litter and should be taken into account [16]. One way to solve this issue is by creating a device or modifying the current rescue hoist system to prevent spinning. Such a device can reduce the rescue duration and remove a danger posed to the helicopter crew and patient. This problem is prevalent in both military medevac and all air ambulance operations and requires further research.

The current technique used by rescue crews to halt litter spin is to emplace a medic on the ground. The medic pulls on a tagline (rope) that is connected to one end of the hoisted litter as shown in Figure 2. In most cases, the tension on the tagline is effective at reducing the spin; however, there have been cases where the tagline broke or became a danger to the helicopter.

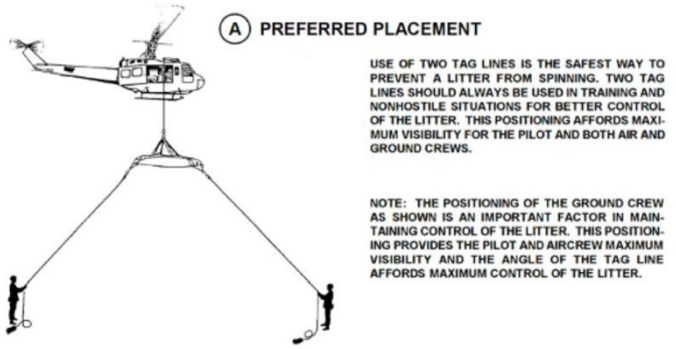

FIGURE 2: U.S. ARMY PREFERRED PLACEMENT OF TAGLINES [19]

For the military conducting medevac operations, a tagline adds additional tactical constraints. As seen in Figure 2, a soldier is lowered to the ground with the litter and must remain underneath the patient holding onto the tagline until the patient enters the cabin [19]. This approach solves the problem of light spin but could not prevent the extreme case that occurred recently in Arizona where the tension broke the tagline [2]. The addition of a medic to hold the tagline further extends the duration of the rescue and increases the exposure of the helicopter to enemy fire. In a hostile environment, the use of the tagline requires more friendly forces to secure the medic on the ground.

Other methods to slow air ambulance litter spinning include flying with moderate airspeed to streamline the litter into the wind or simply lowering the litter to the ground and trying again [16]. Too often, taglines and these alternate solutions are either ineffective, time consuming, or put personnel at further risk [20].

1.3 Designing Towards a Solution

The U.S. Army's 160th SOAR routinely trains and executes air rescues that encounter litter spin. In a series of customer interviews, they indicated their need for a litter stabilization to reduce risk to rescuers and patient, shorten the duration of rescue, and eliminate the need for personnel to hold a tagline. Operators sought a device that was durable, generally light, compact,

affordable, and safe. Application of a design process taught at the U.S. Military Academy defined this problem and then generated a Quality Function Deployment (QFD). The QFD and process translated the customer requirements into key engineering specifications. The resulting engineering specifications were to create device that is affordable (less than $2,000 per unit), efficient (less than 10 seconds settling time), lightweight (less than 30 kg), safe (generated at least 5 N-m of counter-torque), and simple (<10 components). The system was not to exceed the cabin dimensions for the HH-60M, must produce the torque necessary to stabilize the worst-case scenario, and keep the distance between the bottom of the litter and the flywheel under 6 inches [21].

Extensive pilot interviews were conducted as part of the background research. In a typical medevac rescue, oscillation is addressed manually [15]. Table 2 lists some constraints of a typical medevac rescue [15-16], [22-25].

TABLE 2: TYPICAL MEDEVAC RESCUE [15], [16], [22-25]

Constraint	Typical scenario
Tag lines	Usually a secondary tag line is attached to the casualty on the ground to limit rotation
Desired hoist angle	2 to 5 degrees
Hoist distance	20 feet
Extraction time	16 seconds
Reel out and reel in	45 seconds
Time to stabilize the cable	16 seconds
Elimination of static discharge	"The load must touch the ground before the ground crew can handle it" [3]
Maximum counter-torque (estimated)	$5\ \mathrm{N-m}$

The focal point of a solution was to minimize the angular velocity of the litter to ensure the safety of the aircraft, the patient, and the crew chief during hoisting of the litter. This paper presents the design and analysis of a new proposed detachable flywheel device that can be added or removed from any standard air ambulance litter. This paper investigates the design space of defined by angular speed, mass moment of inertia, and flywheel radius that generates the minimum anti-torque. Video analysis of this severe case revealed that the rotor wash generated 5 N-m of torque for up to 10 seconds. The paper also presents the design mechanical models, control theory and necessary gains, and electrical diagrams to achieve the required anti-torque up to severe cases. Custom programming ran a PID controller that signaled a motor controller to direct appropriate voltage to a reversible DC motor. The system was completely self-contained and attached to the underside of any airworthy litter through a series of quick connect buckles. The device had a compact profile to ensure easy maneuvering in and out of the cargo door of the H-60 Black Hawk helicopter.

A device that stabilizes litter spin has many benefits. First, with the flywheel attached to the bottom of the litter, an additional medic or soldier is no longer needed to move into a danger zone on the ground to hold a tagline. Second, there is no need to lower the litter a second time to retrieve additional personnel from the ground. This saves valuable time. Third, the flywheel device is designed to mitigating the worst-case scenario as presented in the Piestewa Peak case. A detachable flywheel device solves the current issue of litter spinning more efficiently and effectively than current methods, while remaining in the confines of customer requirements established by the 160th SOAR.

1.4 Design Considerations

The proposed design had several first and second order considerations to be taken, specifically, in the societal and technological categories. In the societal side, the design impacts the outcome of hoist rescue operations for both military and civilian populations). There have been several injuries or deaths because of hoist rescue operations and the design seeks to mitigate those instances by providing a means to control the dangers that can occur in a medevac rescue. This design has the potential to change the negative connotation that surrounds helicopter rescue operations.

On the technological side, the design has the capability of impacting how current rescue operations are conducted, specifically in the Army. Cyclic loading must be taken into consideration when regarding this device. Understanding the forces and stresses present as the device undergoes uses completely impacts the flywheel device's potential lifetime. The device must be able to withstand the high forces sustained during medevac operations and must be made of strong enough materials to increase overall lifetime of the product.

1.5 Literature Review

Through a literature review and a series of interviews with subject matter experts, the team realized several conclusions that guided the design.

Interviews conducted with pilots and crew of 160th SOAR [15, 16, 20, 23, 24] defined the problem. While the group initially intended to stabilize the sway of a hoist load the pilots expressed more worry about litter spin. In their experience, the sway or swing of the hoist is relatively controllable with pilot inputs to the aircraft controls and with crew chief manipulation of the hoist control. Instead, the crews identified litter spin as the larger concern because the air crew has less ability to stop a spin.

An interview of Dr. Cicolani at San Jose State University Foundation (San Jose, CA) and Ames Research Center (Moffett Field, CA), also gave information on possible methods of stabilizing the spin of a load at the bottom of a hoist [26]. He shared methods used in the past to stabilize Conex's in a sling load system with a swivel connection [26]. Past attempts used passive fins and flexible sails to stabilize the spin of sling load [27]. However, such methods only work in forward flight where there is sufficient free stream velocity. Another approach

suggested by Dr. Cicolani was the use of pressurized air as thrusters to impart a counter-torque.

Multiple patents were reviewed during background research. One patent described the Load Stability Systems (LSS) by Vita Inclinata Technologies [28]. The LSS attached to the sling load cable and used thrust to counteract unintentional rotational motion. It is a temporary and fully automated device with sensory systems, inertial and orientation measurement systems, and control and communication transmitters. Although the device successfully counters the angular momentum of a spinning load, it cannot be used for the current Army standard medevac hoist cable. One of the limitations of the design of the Army standard medevac hoist cable is that any rotational movement will unwind the many strands of the cable and decrease the cable's loading capacity. Rescue hoists use free-spinning hooks to prevent the hoist cable from unwinding; thereby rendering the LSS system incompatible with rescue hoist operations. Still, the concept was novel and showed promise. Vita Inclinata is one of ten finalists in the xTechSearch 4 Finals competition sponsored by the Assistant Secretary of the Army; as one of the finalists, Vita will be presenting and conducting a 'proof-of-concept' demonstration of LSS-LA [29].

To preface this research, a patent created by Breeze-Eastern Inc. of a general hoist system was also reviewed. The benefit of reviewing this patent was to familiarize the team with the industry standard for a hoist system which helps further constrain the design [30,31]. The patent described, in general terms, the components of a hoist system to include: a cable with a controller on one end and a hook on the other. This also includes possible improvements to the simple design, some of which have application to the project. Augmentations to the hook such as a device that measures relative rotation of the hook to the cable present direct relevance to adjusting the spin of a litter. Other points of improvement that might be applied to other hoist systems present constraints that must be considered if the design is to be applied to multiple hoist systems.

A research group from the Georgia Institute of Technology and Stanford University pursued a solution to the same problem of a spinning litter. The graduate team described SALUS (Stabilizing Aerial Loads Utility System as an "electromechanical stabilization system that uses flywheel technology for safer aerial transport. The innovative device can stabilize a hoisted load in seconds, significantly reducing the time needed to perform a potentially life-saving aerial hoist". [32] Their design is promising as it was able to stabilize a spinning litter. The design proposed in this paper is distinguished from SALUS by incorporating the device directly to the litter instead of on the rescue hook like SALUS. Attaching to the underside of the litter has two advantages: (1) the device is easier to remove and attach while not restricting access to the patient; (2) the device applies the counter-torque directly to the litter where control response is desired. Additionally, a larger flywheel (and mass moment of inertia) is possible to the dimensions of the litter.

2. MATERIALS AND METHODS

This section will focus on the derivation of the equations of motion, the development of two different control strategies, and then the behavior of the system with and without the control application. Additionally, the discussion will include analysis of the design space in terms of sizing the motor and flywheel.

Important attributes of the desired outcome are a system that is light-weight, self-contained, modular so that it can be strapped on and quickly removed, and safe. Since the litter rotates in a single plane and such rotation also provide gyroscopic stability. As such, the focus on the design is simply to counteract the spinning motion of the litter in the plane of rotation.

By using a flywheel powered by a motor, it is possible to stabilize the spin rate of the litter through the conservation of angular momentum. By providing a torque that is imparted opposite to the direction of the spin of the litter, it is possible to arrest the motion. However, this is only possible if the flywheel and the motor are sized properly to achieve the required counter-torque to stabilize the litter. For this reason, the governing equations of motion are used to properly size the entire system.

2.1 Governing Equations of Motion

The development of the equations of motion used the Newton-Euler approach to the dynamics problem. The problem focused on the spin rate and angular displacement of the litter about the y axis of the litter in the direction of rescue cable, which yields a single degree of freedom system depicted in Figure 3.

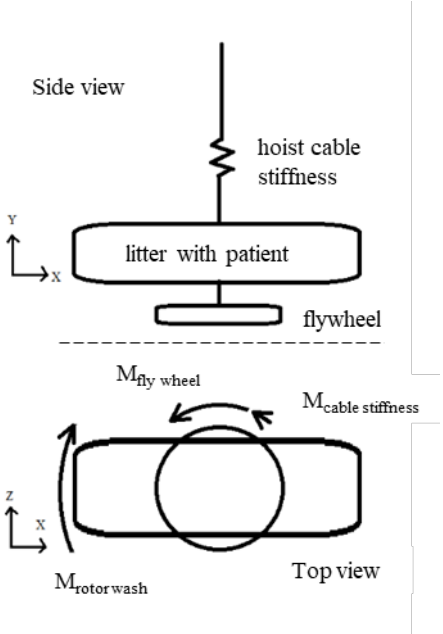

FIGURE 3: FREE BODY DIAGRAM OF THE LITTER-HOIST SYSTEM

Euler's second law, which governs the rotational dynamics of a system in motion, has many forms of varying complexity.

For the purposes of this study, Eq. 1 presents the governing equation for the litter-hoist system.

$$\boldsymbol{M} = \boldsymbol{r}_{cm} \times \boldsymbol{a}_{cm} + I\boldsymbol{\alpha} \tag{1}$$

where $\boldsymbol{M}$ is the total moment, $\boldsymbol{r}_{cm}$ is the position vector from the center of mass to the location where the moments are summed, $\boldsymbol{a}_{cm}$ is the acceleration of the center of mass of the system, I is the mass moment of inertia of the system and $\boldsymbol{\alpha}$ is the angular acceleration of the system. In restricting the analysis to a single degree of freedom, and assuming that the center of mass is co-located with the center of rotation, Eq. 1 becomes the scalar equation $M = I\alpha$.

This approach aims at stabilizing the spin of the litter through conservation of angular momentum. If there is no external torque acting on an object, then there will be no change in its angular momentum. A flywheel system exerts the needed counter-torque to the litter. The equation for angular momentum is,

$$L = I\omega. \tag{2}$$

From inspection of this equation, two major factors play a role in the angular momentum of the system. The first is the mass moment of inertia. The larger this parameter is, the larger the counter-torque imparted on the litter will be. Since the flywheel can be modeled as a hollow cylinder, it is favorable to concentrate the mass on the outer rim of the flywheel, such that the equation can be written,

$$I = \frac{1}{2}m(R_o^2 + R_i^2). \tag{3}$$

If the distance between the outer and inner radius is increased, meaning the rim is thicker, then there would be more mass towards the center of the flywheel which is unfavorable. Having mass in the center or near the center of the flywheel does not contribute much to generating the most torque possible. However, if the distance between the two radiuses are decreased, most of the mass would be located on the outside of the flywheel, allowing for a larger mass moment of inertia seen in Eq. 3.

2.2 Design Space Considerations

To size the motor and flywheel, variables such as mass moment of inertia, radius, angular acceleration, angular velocity, and torque were manipulated through their relationships. Since the motor selection is guided by the size and parameters of the flywheel design, the flywheel design space consideration came first. From a video analysis conducted on the hiker being rescued from the Arizona desert, an average torque of 5 N-m is imparted on a litter by the rotor wash component of a helicopter rotor blade system. An array of mass moment of inertia ranging from 0.14 to 1.48 kg-m^2 is used with Eq. 1 to find the angular acceleration required of the flywheel to provide a counter-torque of 5 N-m. In aircraft systems, weight is essential as it affects its performance parameters such as range and endurance. The flywheel weight can be calculated using the mass moment of inertia I and the sizing requirements given by the Army helicopter pilots. To find the required angular velocity at which the flywheel must spin, a run time of 5 seconds is established. This run time is best explained as the time the flywheel will spin as soon as it is activated by sensory movement. A longer time would require a motor with a higher top speed. After the motor reaches its peak angular velocity with no more acceleration, it cannot anymore counter-torque. Therefore, 5 seconds is chosen as a reasonable timeframe for the motor to run for after being activated. To find the required angular velocity for the motor, Eq. 4 below is used.

$$\omega = \alpha t \tag{4}$$

The final equation that links the flywheel with the motor is:

$$P = \tau\omega. \tag{5}$$

Eq. 5 is the power required by the motor to generate the desired torque at a given flywheel speed. The flywheel design consideration introduces a trade-off between power required and mass. As mass increased, the mass moment of inertia increased. A larger moment of inertia required less angular acceleration to produce the same 5 N-m of torque. The lower acceleration acting over 5 seconds yielded a smaller top angular velocity. From Eq. 5, the power required decreased by the lower top angular velocity. Figure 4 displays the relationship between mass, moment of inertia, and required motor power given a constant torque of 5 N-m. The optimal design point was determined based on sizing requirement for the flywheel and motor power. For a very light flywheel, the power required by the motor would be at its highest, requiring a powerful and heavy motor. On the other hand, a very heavy flywheel needs a small, lighter motor.

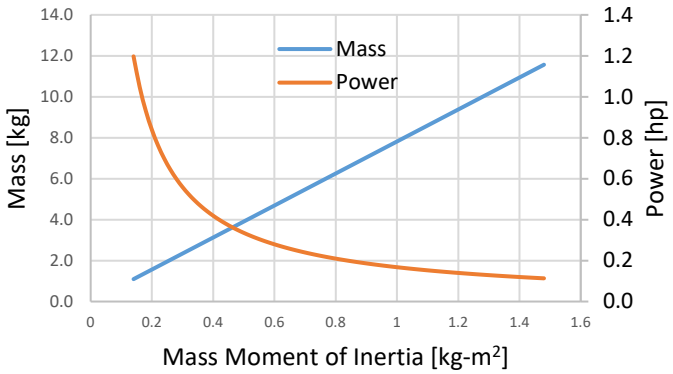

FIGURE 4: TRADEOFF BETWEEN MASS AND POWER

It was discovered that motor weight grew faster than flywheel weight; therefore, a smaller motor with a larger flywheel achieved the desired counter-torque at an overall lower weight.

2.3 Derivation of Equation of Motion for Controller Design

The motion of the litter was modeled as a second order differential equation. To successfully model this system, several assumptions were made. First, the litter was considered to be a flat, rectangular plate. The mass moment of inertia about the center was only affected by the length and width of the litter, making it independent of the thickness. Secondly, the mass moment of inertia was comprised of a lumped mass consisting of both the litter and the person's mass because the mass center was aligned along the axis of rotation. Applying the moment balance law to the system depicted in Figure 3 yielded Eq. 6, where θ and its derivatives are the angular displacement, velocity, and acceleration of the litter.

$$I_G\ddot{\theta} + k_\theta\theta = M_{dist} + M_{cont} \tag{6}$$

The system had three primary torques that cause the litter to spin: the torque caused by external disturbance M_{dist}, the torque provided by the controller to the flywheel M_{cont}, and the torque that arises in rotation due to the (small) rotational stiffness of hoist cable, $M_{cable} = -k_\theta\theta$. The spring constant was estimated to be 0.05 N-m/radian. The mass moment of inertia of the litter-patient lumped mass was calculated based on an assumed homogeneous distribution of mass around the volume of a rectangular prism equal to the size of the litter. In this study, the mass moment of inertia of the litter-patient was a constant I = 27.3 kg-m^2.

Rotor downwash is the primary source of M_{dist}. The flow field that generates the moment is complex. The torque found through the video analysis of the Arizona medevac rescue of 5 N-m is assumed to be a constant torque, which is used as M_{dist}.

2.4 Controller Design

A controller was designed using two different methods: classical Proportional-Derivative (PD) control and full state feedback control. The objective of most control design is to achieve stability, eliminate steady state error, and optimize transient response. Likewise, this section evaluated the conditions for stabilizing the angular displacement, θ, of a litter using a root locus approach. Settling the angular displacement rather than velocity allowed for greater simplicity of the controller. As will be discussed later, the exact angle of the litter once settled was irrelevant if its angular velocity was zero. This permitted a lower level of accuracy demanding fewer regulating terms in the controller design. In addition to making the design process easier, it allowed for more rapid iteration to adjust the influence of those regulating terms.

2.4.1 Controller Design via Root Locus

Eq. 6 is linear and was well-suited to direct application of various linear, classical control techniques, including Proportional-Derivative (PD) control. A PD controller compared information about the error and the error rate to generate a control response. Each term's influence on the output was further regulated by a gain, represented as K. Proportional control was the simplest and calculated a control effort (CE) based on the error. This type of controller is typically enhanced by adding derivative element to prevent overshoot. By comparing the rate of change in error correction, the derivative controller throttled the transient response by decreasing the CE as it approached the setpoint. It is also common to add an integral term, forming a PID controller. The intent behind this term was to reduce steady state error by ensuring the CE remains above zero until the set point was reached. In this instance, only a PD controller needed to be implemented. The integral term was neglected due to the irrelevance in reducing steady state error in the defined system. A steady state error was deemed acceptable because the output was defined as angular displacement which implies that an error translates to a difference in orientation of the litter. If the error was steady, the angular velocity had been eliminated, and it would not be advantageous to return the litter to an angular displacement of θ=0 radians.

A PD controller was designed in the Laplace domain. The transform is applied to Eq. 6 and plotted on a root locus. The transformed equation was:

$$\tau(s) = (Is^2 + k_\theta)\theta(s) \tag{7}$$

The torque function τ(s) remained a constant value. This allowed modelled as a step input which, after being transformed, equaled:

$$\tau(s) = \frac{5}{s} \tag{8}$$

The output variable θ(s) was the basis for the root locus and was isolated. After combining Eqs. 2 and 3, the result was:

$$\theta(s) = \frac{5}{s(Is^2 + k_\theta)} \tag{9}$$

The root locus of Eq. 10 demonstrated the instability of the system. Poles were determined by the roots of the denominator and found to be 0 and $\pm 0.1353i$. This demonstrated that the system was marginally stable as defined by the poles strictly on the $j\omega$ axis. To eliminate the rotation rate, a controller needed to be implemented.

The desired system properties were established as having 5%OS and a settling time of t_s = 5s. Because the system has two poles, the resultant PD controller required two zeros to pull the traversals of the poles out of the right-hand plane. These zeros had to satisfy the angle criteria and the magnitude criteria of a root locus to be included in the closed loop transfer function. After implementing the PD controller, the root locus was depicted in the complex plane of Figure 5 and was:

$$G_c = 8.49(s + 0.3)(s + 0.639) \tag{10}$$

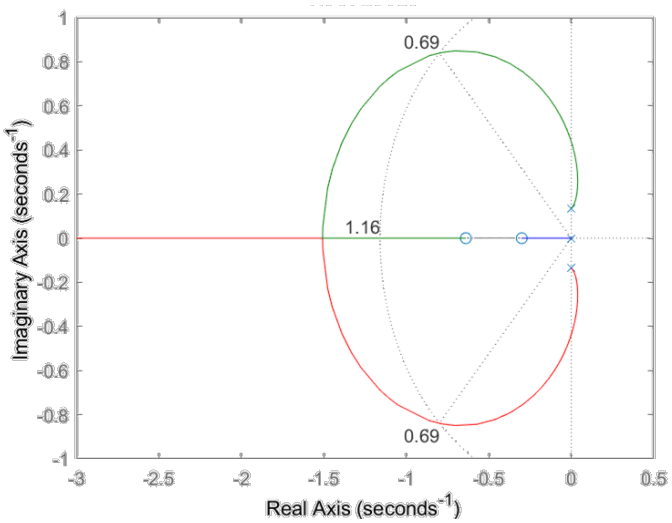

FIGURE 5: ROOT LOCUS OF COMPENSATED SYSTEM

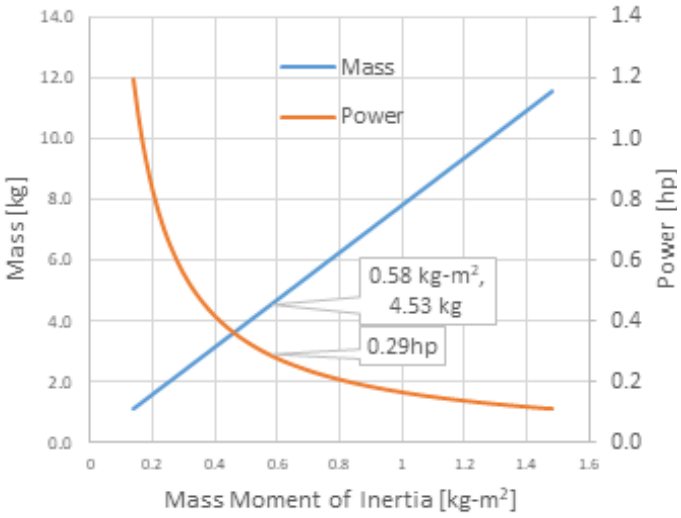

FIGURE 6: TRADE-OFF BETWEEN MASS AND POWER

2.4.2 State Feedback Approach

To design a controller based on state feedback, it is customary to identify the states and then place the system in first order form. The states were selected as $x_1 = \theta$ and $x_2 = \dot{\theta}$. Rearranging Eq. 6 and making the necessary substitutions yields Eq. 11.

$$\dot{x}_1 = x_2$$
$$\dot{x}_2 = \frac{M_{dist}}{I_G} - \frac{k_\theta}{I_G} x_1 + \frac{M_{cont}}{I_G} \qquad (11)$$

To stabilize the system, the counter-torque produced by the flywheel was modeled as M_{cont}. A control law was needed to determine the amount of counter-torque. The error vector was the desired state $\boldsymbol{x_d}$ minus the state at any time t per Eq. 12.

$$\boldsymbol{e}(t) = \boldsymbol{x_d} - \boldsymbol{x}(t) \qquad (12)$$

The control law set $M_{cont} = \boldsymbol{Ke}$, where $\boldsymbol{K}$ is a 2×1 vector of control gains [k_1 and k_2], and M_{cont} was therefore a scalar value of torque. For the purposes of this study, $\boldsymbol{x_d}$ = [0 0], i.e. zero angular displacement and zero angular velocity.

3. RESULTS AND DISCUSSION

The final design needed was a compromise of flywheel mass and motor power. The flywheel design point was a mass of 4.53 kilograms and a power requirement of 0.29 hp. This selection was determined as a satisfactory compromise between mass, size, and motor availability with the idea to reduce overall weight (sum of flywheel weight and motor weight). Figure 6 highlights the design point over the trade-off between mass and power of the flywheel. The selected design characteristics were labeled to show the relative distance from the optimal design.

The intersection point laid at a mass moment of inertia of 0.48 kg-m^2 and a power requirement of 0.35 hp. This location characterizes the optimal properties a flywheel should possess to minimize both mass and power required to generate the necessary counter-torque. However, a lack of motors available in the optimal power range with the necessary maximum rotation speed posed an additional constraint to selecting design properties. Instead, the closest approximation to the intersection point was selected based on the performance of available motors. The chosen motor, generating 0.29 hp up to a maximum speed of 500 rpm, therefore demanded a larger mass to produce the necessary torque.

Equally important to designing the final product was determining an effective controls model to regulate the counter-torque response. Both the state space and root locus approaches provide advantages with their analysis however, the root locus model is more applicable to performance analysis and coding design which made it the better choice for designing a controller. The root locus was a powerful tool for creating the necessary counter-torque in the design space. The two approaches started with identical equations of motion and yield correct, but different results.

The state space approach examined the effect on litter displacement and velocity by tuning gains values. These gains interacted with the litter response as controls to either position or velocity. These were adjusted to generate a new response which was visually analyzed using the plots of angular displacement and velocity with respect to time. The approach was unique in its simplicity to model the system of interest. Gains were easy to adjust allowing for new response solutions to be generated in very short succession. This was especially important as the performance of the system was analyzed after the gains for the controller were already selected.

The root locus approach utilized the differential equation of motion after in the Laplace domain. From these equations, a visualization of the response in the Laplace domain was used to construct an ideal response based on calculated values from the design requirements such as settling time and percent overshoot. This, while taking more time to model one solution, always

results in a controller that achieves the exact performance results demanded. The versatility of this tool makes its use a significant asset compared to the alternative approach. Accuracy and ease of modelling are important considerations because there always exists a gap between the device's modelled and actual performance that makes redesigning the controller an inevitability.

To achieve the optimal response from the device, an analytical approach to improving the controller was imperative and using the root locus approach reduced the barrier to redesign. The main advantage was the accuracy of desired performance characteristics. While the state space approach designed a controller based on different gains in rapid succession, the result had to be analyzed to ensure that it produces a viable response. The controller was only an approximation of the ideal performance as a result; a problem that was only exacerbated when applied to a real system. Although the root locus approach takes more time to generate, the accuracy of the final product made its use an imperative.

3.1 Design Products

The finalized design reflected the engineering analysis and the customer requirements outlined in previous sections. The motor and flywheel were the primary constraints around which the supporting device as shown in Figure 7. The CAD model shown in Figure 7 is the completed design with its components in addition to their locations on the design.

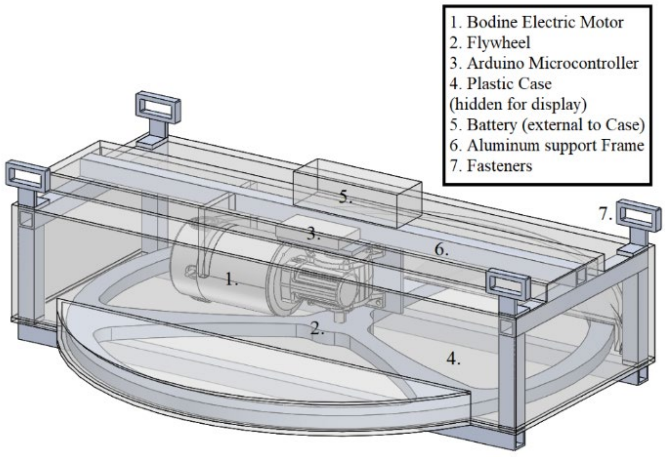

FIGURE 7: CAD MODEL OF THE FINALIZED DESIGN

The final design generated the necessary 5 N-m of torque when accelerated at a rate of 53 rpm. Maintaining a diameter of 0.76 m, it was slightly larger than the width of the litter. This compromise was tolerated in exchange for weight reduction. Because the mass moment of inertia of a generic object is a product of its mass and the square of its distance from the center of rotation, increasing the diameter had an greater effect than mass on the flywheel's performance. This made a more weight efficient design which was a key attribute for an aircraft system.

The motor provided the greatest constraining factor on the design. AC motors were less appealing because they required the additional weight and complexity of a converter. DC motors were examined to complete the design. The chosen motor, created by Bodine electric company, is a right-angle gear motor that accepted a 24V, 17A DC input. Its maximum angular velocity was 500 rpm which allowed the device to generate the average torque necessary for up to 10 seconds. The motor weighed 16.8 lbs making it a significant part of the system's overall mass.

3.2 Design Point Discussion

The device was successful in meeting some of the target values but failed to meet others. Priority was given to satisfying the most important engineering characteristics as these dictated the device performance most heavily. Table 3 characterizes the target values and the device's success in attaining them. Each engineering characteristic is listed 'A' through 'F' in order of importance and labeled if the value was exceeded, met, or unmet.

TABLE 3: ENGINEERING CHARACTERISTICS AND TARGET VALUES

Engineering Characteristic		Units	Target Value	Actual Value	Outcome
A	Counter-Torque	N-m	5	5	Met
B	Settling Time	seconds	10	10	Met
C	Number of Parts	quantity	10	6	Exceeded
D	Unit Weight	kg	23	28	Unmet
E	Unit Cost	US $	500	1900	Unmet
F	Footprint	m^2	0.186	0.483	Unmet

The design process resulted in satisfying the highest rated engineering characteristics at the expense of the lower priority targets. The counter-torque dictated the effectiveness of the device in arresting the litter's spin. The achievement of this target was imperative before any other. This inherently conflicted with the desire for low weight and small area due to their role in utilizing acceleration to generate a torque. Likewise, these two engineering characteristics suffered from large margins of error to their target values to accommodate the torque. Similarly, the settling time was important to settle the litter within a duration that was useful for hoist rescue operations and safe to the patient. Settling time was independent of the other metrics.

The most significant difference between the target and actual value was the price, being constructed nearly 280% overbudget. This as well as the other failures were largely explainable through the novelty. The target cost value was for a prototype only and did not account for production efficiencies.

3.3 Motion of Uncontrolled System

Equation 6 described the motion of the litter with a single constant torque applied and the simplifications above applied. The resulting motion was in Figure 8, which depicted a typical second order response plot. The angular displacement grows rapidly due to a very small cable stiffness; in a minute, the litter

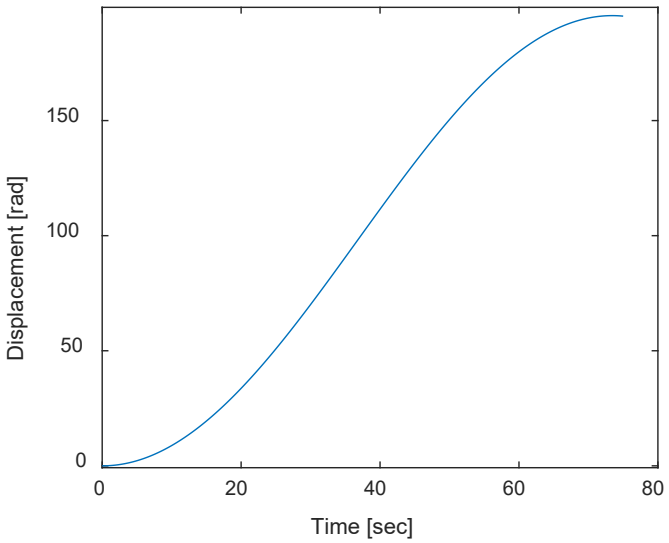

FIGURE 8: UNCOMPENSATED RESPONSE OF LITTER TO A CONSTANT TORQUE

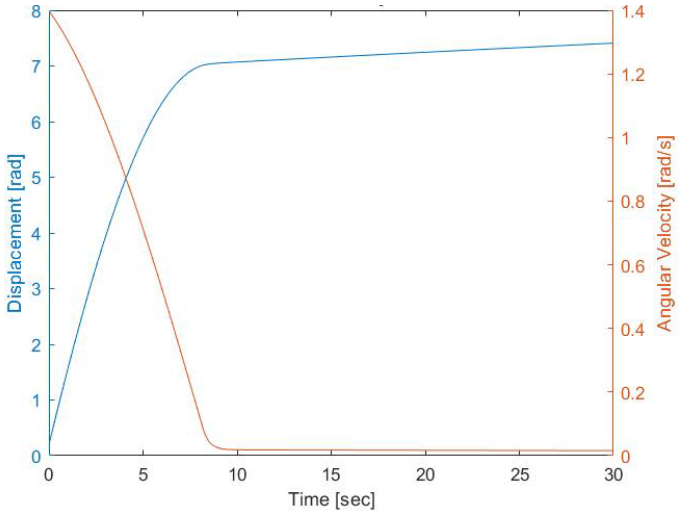

FIGURE 10: CONTROL USING STATE FEEDBACK

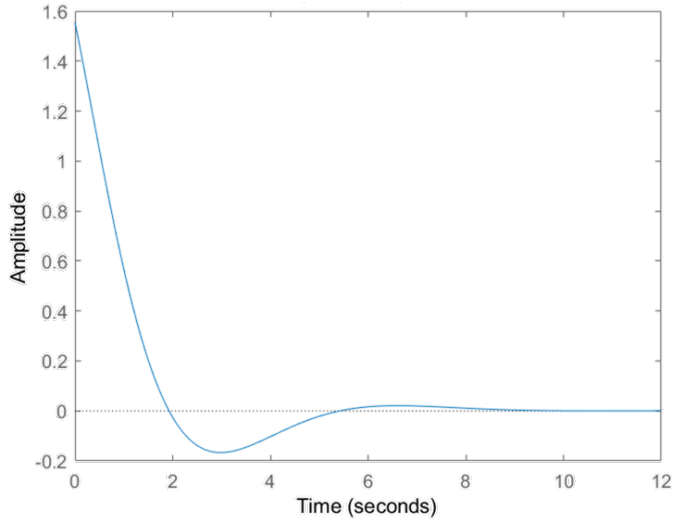

FIGURE 9: IMPULSE RESPONSE OF P-D CONTROLLER

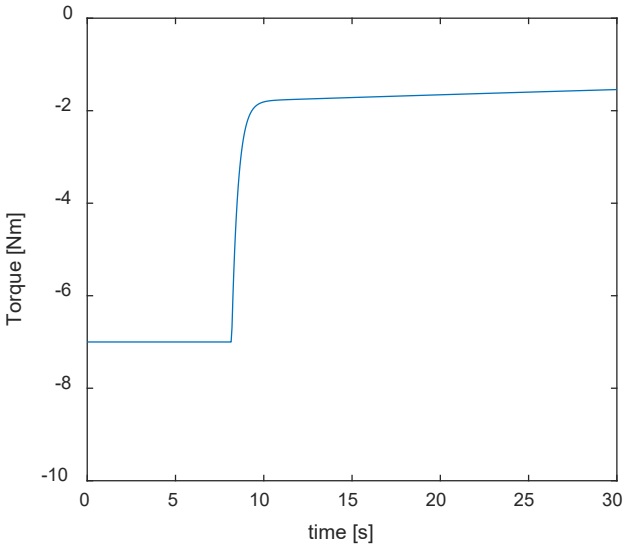

FIGURE 11: TIME HISTORY OF TORQUE FOR SATURATED CONTROLLER

made over 30 revolutions, with a top speed of almost 1 revolution per second. Eventually, the stiffness of the cable countered the external torque of the rotor wash, and the rotation rates slowed, and ultimately reverse. Without a damping term, the system was marginally stable and oscillated infinitely once disturbed from equilibrium. This system required active control in order arrest the spin rate and allow for safer operation.

3.3.1 Classical PD Control Results

Based on the controller designed in 2.4.1 and Eq. 10, the zeros selected for this controller satisfied both criteria mentioned above and achieve the desired response. The controller was effective with an impulse to the system and an applied external torque. Rather than oscillating infinitely like an uncompensated system, the designed controller behaved much differently as shown in Figure 9. The system settled into a steady state at the desired time of five seconds and exhibited a 5% OS as designed. Implementing the PD controller resulted in an effective arrest of the angular velocity in the simulated environment; however, this linear control strategy was not able to adequately model nonlinear effect such as control saturation. Since saturation was a concern, full state feedback was used as a point of comparison.

3.3.2 State Feedback Control Results

In addition to the classical controller, a state feedback controller was designed, as described in 0. The gains from the controller are k_1 and k_2, which determined the sensitivity of the

feedback controller to the error in the angular position and angular velocity, respectively. Depending on the gains, it was possible to observe system behavior by looking at a time history of the displacement and angular velocity of the system. The spin rate was detected by an onboard inertial measurement unit; angular displacement, however, was more difficult to determine robustly. Therefore, the best results were achieved when k_1=0 and k_2=75, which are depicted in Figure 10. This simulation also assumes that the motor-flywheel is not able to deliver more than 7 Nm of torque at any given time.

In Figure 10 the velocity was brought to almost zero within 10 seconds. There was a very small increase in angular displacement at this point, with an increase in angular displacement of approximately 17 degrees in 10 seconds. This is well with the needed safety parameter to complete a hoist to the helicopter fuselage. A slow spin of this magnitude can be safely caught by the crew chief as the litter is brought into the cabin. The time history of required torque was provided in Figure 11.

3.4 Stress and Engineering Materials

To evaluate the performance of the designed flywheel device, a study of the material strength was conducted using SOLIDWORKS simulation software. The purpose of modelling the flywheel was twofold. Due to the high rates of rotation the flywheel device must undergo, a material failure invited the possibility of severe injury or damage to the aircraft in testing. The analysis evaluated the stresses at various angular speeds and drove the material selection and component thickness. The secondary purpose for simulating the flywheel was to enable future innovation in the design. The simulated stress at different locations aided in understanding where the design could be refined to reduce inefficiencies.

The flywheel was evaluated in two scenarios: acceleration from a resting state and deceleration from a maximum angular velocity. This was accomplished in SOLIDWORKS by applying a centrifugal force on the rim of the flywheel such that the maximum change in angular velocity was considered. By simulating the stresses of the flywheel at these extremes, potential locations of failure could be identified. Figure 12 and Figure 13 illustrate the results.

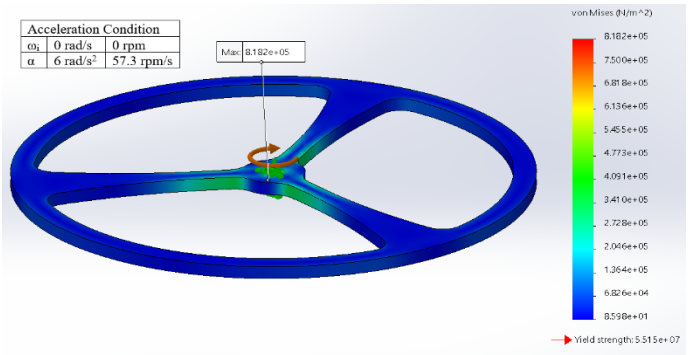

FIGURE 12: MAXIMUM ACCELERATION FROM REST

The first simulation considered an acceleration of 6 rad/s^2 from rest with the intent of mimicking the maximum response to an abrupt change in angular velocity. Stress was found to be most intense at the keyhole where the motor shafted mated with the flywheel. Despite this stress concentration, the factor of safety between stress and the material yield strength was far greater than necessary at 67.4. The extreme nature of this value informs future iterations of the design where mass can be reduced with minimal change to moment of inertia. While the region directly contacting the motor should not be changed to prevent increasing the stress on this mate, the surrounding portion of the collar and the inner spokes can shed mass to decrease weight.

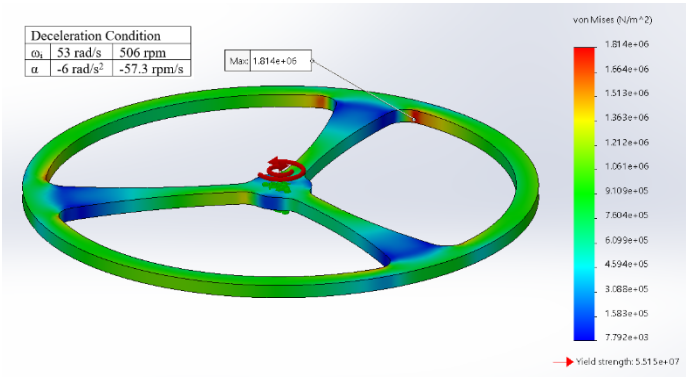

FIGURE 13: DECELERATION FROM PEAK SPEED

In the second scenario, the flywheel was decelerated from the maximum angular velocity of the motor by a rate of 6 rad/s^2. Like the first simulation, the change in angular velocity was the maximum rate allowable for the intended operation time; however, unlike the former, the greatest stress on the flywheel was located where the spokes merged with the outer rim. The cause of this can be surmised to be a stress concentration where the centripetal force of the local mass element pulled on a region of decreasing area. An explanation to the differing location of stress from the first simulation was the flywheel inertia to maintain angular velocity. For any given section, the mass's momentum is tangent to the point furthest from the center of rotation. This, as opposed to the first case, contributes to the stress encountered on the outer rim significantly. Regardless, the factor of safety for this case was still well above conventional design parameters at 30.4, again showing where the design my achieve better weight efficiency.

The resultant stresses in both cases were below the yield strength of the aluminum used. This informs future designs in two different ways. One possible use for the information is weight reduction. As discussed earlier, locations such as the inner part of the spokes are inefficient in their use of material. This area contributes little to the flywheel's mass moment of inertia, a product of both the mass and distance from its center of rotation. This reduced mass is critical consider for future prototyping as weight was a design requirement that was not met. Alternatively, the flywheel can be modified to increase its mass moment of inertia, thus reducing the acceleration needed from the motor. Such a change, though affecting many other

considerations for the device including motor selection, device footprint, and overall mass, would lead to a far superior design that comes much closer to meeting design criteria and yielding a useful product for the user.

3.5 Logistical and Economic Results and Analysis

Table 4. summarized the cost of materials of a single prototype flywheel device. In total, this project cost $5,960 out of the initial budget of $10,000. These costs included multiples of each material or device in the manufacturing process as well as a Stoke's litter and straps. The resulting cost to manufacture one single device was about $1,900. Not included in the cost to manufacture a single unit are extras such as battery chargers or a Stoke's litter. The estimated $1,900 could also easily be reduced in the future through bulk purchases.

TABLE 4: COST OF A SINGLE UNIT

Item	Cost
IMU and Arduino	$115
Motor controller	$281
Motor	$592
Wires	$33
Voltage regulators	$8
Flywheel	$676
Frame material	$191
Total Cost	$1,896

4. Conclusion

This project analyzed various solutions to stabilize the spin of a rescue litter in air ambulance operations. Litter spin is a common issue during military medevac operations caused by the helicopter blade's rotor wash. The spin jeopardizes the timeliness of the mission and the safety of the aircraft, the aircrew, and the patient. Similarly, a spinning litter results in more time required to stabilize and pull the litter into the helicopter cabin which leads to more exposure to enemy fire and increased danger.

Unlike current methods of halting litter spin through the utilization of a medic on the ground, this project stabilizes the spinning of a litter through a safer and more efficient mechanical approach. Specifically, this project explored the impact of providing a counter-torque by attaching a flywheel controlled by a PD controller to the bottom of a medevac litter. The specified device is held in a durable, lightweight enclosure. Within the enclosure, a flywheel is mounted to a DC motor and electrically connected to a motor controller, a battery, an Arduino processor, and an inertial measurement unit (IMU) device. Ultimately, through guidance from the 160th Special Operations Aviation Regiment (SOAR), this device was designed to meet all given sizing and weight requirements as well as drastically increase the safety of air ambulance medevac operations.

ACKNOWLEDGEMENTS

The views expressed herein are those of the authors and do not reflect the position of the United States Military Academy, the Department of the Army, or the Department of Defense. This project was sponsored by Bell Textron and supported by the U.S. Army 160th Special Operations Aviation Regiment (SOAR). Breeze Eastern provided valuable technical assistance in understanding the problem and creating a reasonable solution. The authors acknowledge discussions with L. Cheben, P. Gilman, G. Griffiths, L. Cicolani, D. Creech, P. Doyle, J. Fett, C. Hawk, M. Koons, J. Luczkovich, J. McKinley, A. Morock, T. Aldhizer, K. Hughes, and W. Lacarbonara. M. Lanzerotti acknowledges discussions with J. Vanderlip, J. Rahon, C. Schools, J. Ness, D. Schultz, B. Matthews, J. Demarest, P. Chapman, J. Capps, B. Huff, J. Medeiros, I. Azeredo, B. Novoselich, J. Whipple, S. Thompson, R. Melnyk, A. Arena, and E. Naessens.

REFERENCES

[1] A. Venosa, "Breaking Point: What's The Strongest G-Force Humans Can Tolerate?," *Medical Daily*, 2016. https://www.medicaldaily.com/breaking-point-whats-strongest-g-force-humans-can-tolerate-369246 (accessed Nov. 19, 2019).

[2] KSAT 12 ABC, "(84) Helicopter rescue of 74-year-old woman goes wildly wrong - YouTube," 2019. https://www.youtube.com/watch?v=Llpii85mzBo (accessed Nov. 19, 2019).

[3] United States. Department of the Army. (2000 April 14). "Medical Evacuation in a Theater of Operations: Tactics, Techniques, and Procedures", U.S. Army Field Manual No. 8-10-6. Washington, DC. FM 8-10-6. Figs. E-3A, B, C (pp. E-18 and E-19).

[4] Helicopter rescue at Pear Lake. 2019. [Online]. Available: https://www.youtube.com/watch?v=lLi2YsYY3j0

[5] Helicopter rescue in Dry Bone Canyon. 2018. [Online]. Available:https://www.youtube.com/watch?v=QMy9e3CKvbw.

[6] Helicopter rescue near Hiawassee. 2016. [Online]. Available: https://www.youtube.com/watch?v=qvsTkYO inrQ.

[7] Helicopter rescue by Air Zermatt. 2016. [Online]. Available: https://www.redbull.com/inten/shows/the-horn

[8] Helicopter rescue near Wilmington, NC. 2018. [Online]. Available: https://www.charlotteobserver.com/news/local/article214847390.html.

[9] Helicopter rescue near Noumea, New Caledonia. 2018. [Online]. Available: https://www.youtube.com/watch?v=6sAIOdnflQ0.

[10] Helicopter rescue in Vancouver. 2019. [Online]. Available: https://www.youtube.com/watch?v=83HfFjBEgcQ.

[11] Helicopter rescue near the Bering Sea. 2018. [Online]. Available: https://www.youtube.com/watch?v=jqWFeYGKhmk.

[12] Helicopter rescue in California from water. 2017. [Online]. Available: https://www.youtube.com/watch?v=D3qESLaGgaU.

[13] Helicopter rescue in Tillamook. 2017. [Online]. Available: https://www.youtube.com/watch?v=eLewQWDY6d0.

[14] MAJ Will Cox, "Georgia medevac training: Very little room for error, [Online]. Available: https://www.nationalguard.mil/News/Article-View/Article/576175/georgia-medevac-training-very-little-room-for-error/. July 22, 2014.

[15] CPT Landon Cheben, "160th SOAR Teleconference 13 SEP." West Point, NY, 2019.

[16] CPT Landon Cheben, "160TH SOAR Teleconference 24 September, 2019." West Point, NY, 2019.

[17] Samuel W. Ferguson, Rotorwash Analysis Handbook. Volume 1-Development and Analysis. U.S.A., Washington, DC, AD-A284 719. Report DOT/FAA/RD-93/31, I. 1994.

[18] D. Richard A. Scheuring, William Rainey Johnson, Geoffrey E. Ciarlone, and F. G. O. Keyser, Naili Chen, Environmental Extremes: Alternobaric Sam Houston, TX: Borden Institute, 2019.

[19] United States. Department of the Army. (2000 April 14). "Medical Evacuation in a Theater of Operations: Tactics, Techniques, and Procedures", U.S. Army Field Manual No. 8-10-6. Washington, DC. FM 8-10-6. Figs. E-3A, B, C (pp. E-18 and E-19).

[20] CPT Landon Cheben, "160th SOAR Teleconference 10 December, 2019." West Point, NY, 2019.

[21] S. W. Ferguson, "Rotorwash Analysis Handbook Volume I-Development and Analysis," Mansfield, TX, 1994.

[22] P. Doyle, D. Creech, Teleconference with Breeze-Eastern. 7 January, 2020, Personal communication.

[23] P. Gilman, Teleconference with U.S. Army helicopter pilots. 8 January, 2020, Personal communication.

[24] L. Gilman, Teleconference with U.S. Army helicopter pilots. 3 March, 2020, Personal communication.

[25] Jeffrey L. Langhout, Director. Aviation Engineering. United States. Department of the Army (2001 Oct 2, 2014 Ay 5/R11). Airworthiness Release (AWR) for Rescue Hoist Equipment on UH/HH-60 Helicopter (AWR 980). US Army Research, Development, and Engineering Command, Aviation Missile Research, Development, Engineering Center, Redstone Arsenal, Alabama.

[26]. Dr. Luigi Cicolani, "Teleconference 4 October, 2019." West Point, NY, 2019.

[27] L. S. Cicolani and M. G. E. Ehlers, "Modeling and Simulation of a Helicopter Slung Load Stabilization Device," 2002.

[28] Vita Inclinata. [Online]. Available: https://vitatech.co/news/vita-showcasing-its-load-stabilitysystems-at-heli-expo-2020/.

[29] Vita Inclinata. [Online]. Available: https://vitatech.co/news/vita-advances-as-a-us-army-xtechsearch-4-finalist/

[30] B. Repp, B. Pedersen, E. Johnson, C. Cariano, C. Dize. *Helicopter Hoist Systems, Devices, and Methodologies*. 17 July 2018. US Patent 10059462.

[31] B. E. Staff, "Breeze Eastern Visit 30 SEP." Whippany, NJ, 2019.

[32] Stewart, J. (2019, September 19). Suturing Device, Helicopter Hoist Stabilizer Make it to Finals of National Collegiate Inventors Competition. Georgia Tech. Available: https://news.gatech.edu/2019/09/19/suturing-device-helicopter-hoist-stabilizer-make-it-finals-national-collegiate-inventors